Hindawi
Shock and Vibration
Volume 2019, Article ID 6086874, 11 pages
https://doi.org/10.1155/2019/6086874

Research Article

Coupling Synchronization Criterion of Two Hydraulic Motors in an Eccentric Rotary Vibration Machine

Chun-lei Luo, Xin Mo, Jin-yang Li, Zhi-qing Tang, and Song-song Huang

College of Mechanical and Electrical Engineering, Central South University, Changsha 410083, China

Correspondence should be addressed to Chun-lei Luo; 134247@csu.edu.cn

Received 13 October 2018; Revised 2 December 2018; Accepted 9 December 2018; Published 20 January 2019

Academic Editor: Angelo Marcelo Tusset

In an eccentric rotating system driven by two hydraulic motors without synchronous gears, vibration coupling may help render motion stable. In order to investigate how vibration coupling influences the motion, the coupling characteristics of the vibration system were studied regarding the differences between two motors such as leakage network, coulomb damping network, and pressure loss network, and the sensitivity of the influence factors was also studied. The influence of tiny differences between the two motors, tiny differences in the motion pair structure, in the oil temperature and in the resistance coefficient on the coupling motion were discovered, and the criterion for synchronous motion were obtained consequently. The results show that the influence of the resistance coefficient difference on system motion stability is the greatest, accounting for 46.7%, and the influence of the difference in motion pair structure (e.g. motor piston clearance) is the second, accounting for 32.8%. For motors with displacement 80 ml/r, the condition of self-synchronization is that the difference in piston clearance between the two motors is equal to or smaller than 6 μm. Experiments have proved the correctness of the theory and showed that the synchronization can be achieved by leakage compensation, damping compensation, and back-pressure compensation of the external system by means of control when the motors rotate slowly enough for system response. The study shows that the coupling synchronous model can reduce the force of the gear for the eccentricity rotary system with synchronous gear, and that the synchronous stability can be improved for the eccentricity rotary system without synchronous gear.

1. Introduction

The theoretical system and technical application of the vibration synchronization and control synchronization of the mechanical system driven by electromotors have long been developed, and even the nonlinear problems of the mechanical system such as vibration stability and bifurcation of self-synchronous systems driven by electromotors have been well solved [1, 2]. However, because of the limited driving capacity of the electromotor-driven system, it is difficult to obtain the application of synchronous vibration and control motor transmission under large loads.

Hydraulic-driven eccentric rotary vibration system is widely used. It is characterized by high power and a large resistance coefficient and stiffness of working object. And, its synchronization is constrained by the synchronizing gear. The problems of the system are as follows: gear driving mechanical structure is too complicated; gears and other transmission parts are prone to damage etc [3]. Field tests show that the coupling effect has a direct influence on the gear stress and vibrating noise of the two rotating systems. The study of synchronization can provide theoretical basis for reducing influences of nonsynchronized factors on synchronizing gear stress, and even for removing the synchronization gears and simplifying the structure.

Reference [4] studied the effects of friction torque, dynamic stiffness, dynamic damping, structural parameters of vibrator, hydraulic motor leakage, and other factors on the stable working process and transition process of the system. References [1, 2, 5, 6] researched and applied coupling synchronization mechanism driven by motors. Reference [7] reported a preliminary study about the basic problems on hydraulic motor-driven synchronization system with small and unchangeable damping coefficient and stiffness, and in the modeling process, electrohydraulic control was neglected. Considering high power and a large damping coefficient, references [3, 4] studied electrohydraulic coupling modeling and simulation about the eccentricity

gyration hydraulic-driven control system, and it discovered that the two motors in the eccentric gyration system possess coupling synchronization performance when the hydraulic system is under certain conditions (such as two systems with the same mass flow of hydraulic oil, hydraulic motors with required divulging differences, gyration systems with required mechanical efficiency differences, foundation soil with elastic stiffness in required range, etc). In reference [8], considering the soil hysteresis characteristics, the influence of working parameters of hydraulic vibration hammer on coupling characteristics was studied. Also, the synchronicity, stability, and sensitivity of the hydraulic vibration hammer without synchronous gear were studied in reference [8], considering the leakage characteristics of hydraulic system.

In this paper, based on the analysis of mechanical-electric-hydraulic coupling characteristics of the two rotating systems in dynamic balance process, the synchronous criterion of steady vibration eccentric gyration hydraulic-driven system was studied considering the factors such as mechanical damping, load damping, hydraulic system viscosity, hydraulic motor motion pair clearance, leakage, etc. In order to avoid the adverse effect of pipeline differences on synchronization, the electrohydraulic proportional valve was directly fixed at the inlet of the hydraulic motor. The coupled synchronous vibration hammer model is shown in Figure 1 [9, 10].

2. Description of the Two Rotating Systems in Dynamic Equilibrium Process

How to achieve synchronous motion of hydraulic motors has been restricting the application of self-synchronization of hydraulic motor in vibration engineering. But, there are more factors affecting the self-synchronization of hydraulic motors than electric motors [11–13], which is determined by the characteristics of the hydraulic system itself, such as flow leakage, large damping, and so on. Our research mainly includes two parts: coupling and compensation. Synchronization criterion is found by kinematic coupling, and the deficiencies of vibration system are compensated by means of control, such as reducing the difference between two hydraulic motors and other parts in the system (manufacturing difference or wear difference after using for a period of time) to meet the synchronization criterion and achieve synchronization. This article mainly focuses on the former (synchronization criterion and its influencing factors).

The hydraulic flow entering the working chambers of the two motors is approximately the same under the action of the flow control valve. As shown in Figure 2, in the working process of two hydraulic motors, when there is a phase difference between the two eccentric rotary systems, the hydraulic motor with advanced phase is hindered by the vibration resistance moment of the hydraulic motor with hysteretic phase, which leads to the increase of the load and causes a deceleration movement occurs on the motor with the advanced phase. Meanwhile, the increase of the load pressure causes the increase of the leakage of the motor; so, the effective working flow of the motor is relatively decreased, which further reduces the speed of motor with the advanced phase. At the same time, the opposite occurs to the hydraulic motor with the hysteretic phase. Simply put, the eccentric rotor with the advanced phase helps accelerate the eccentric rotor with the hysteretic phase, until both reach the same speed. Next, this paper will explore under what conditions the two hydraulic motors can achieve synchronous motion.

3. The Derivation of Coupling Characteristic Solution

3.1. Vibration Coupling Model. The structure principle of inertia-excitation gyration with two motors is shown in Figure 1. The hydraulic power component is quantitative plunger pump. The hydraulic control component is Model BT32, which is a high-pressure and great flow capacity proportion flow valve and is forerunner control type with displacement-electricity feedback. The hydraulic actuator is quantitative plunger motor [3, 14]. It is assumed that the quality of eccentric block, eccentric radius, and moment of inertia in the gyration system is the same. The differences of hydraulic motor leak of each gyration system should not be ignored. Vibration power consumption, damping force, and stiffness of the object should not be ignored [15–17]. The precision of electrohydraulic proportional flow valve is sufficient [3].

Luo [3] studied the coupling relationship about vibrating of the hydraulic-driven system:

$$\begin{aligned}
&\frac{1}{2}mr^2\Delta\ddot{\alpha}_1 + (f_1 - mra_3\omega_{01})\Delta\dot{\alpha}_1 \\
&\quad + mr(a_2\omega_{02}\sin\gamma - a_4\omega_{02}\cos\gamma)\Delta\dot{\alpha}_2 + f_1\omega_{01} \\
&\quad + \frac{mr}{2}\left(a_2\omega_{01}^2\sin\gamma - a_3\omega_{01}^2 - a_4\omega_{02}^2\cos\gamma\right) - \mu_1 P_1 q = 0, \\
&\frac{1}{2}mr^2\Delta\ddot{\alpha}_2 - mr(a_1\omega_{01}\sin\gamma + a_3\omega_{01}\cos\gamma)\Delta\dot{\alpha}_1 \\
&\quad + (f_2 - mra_4\omega_{02})\Delta\dot{\alpha}_2 + f_2\omega_{02} \\
&\quad - \frac{mr}{2}\left(a_1\omega_{01}^2\sin\gamma + a_4\omega_{02}^2 + a_3\omega_{01}^2\cos\gamma\right) - \mu_2 P_2 q = 0.
\end{aligned} \tag{1}$$

In equation (1),

$$\begin{aligned}
a_1 &= \frac{mr\left[\left(k_y - M\dot{\alpha}_1^2\right)\dot{\alpha}_1^2 + \left(f_y\dot{\alpha}_1 + M\ddot{\alpha}_1\right)\ddot{\alpha}_1\right]}{\left(k_y - M\dot{\alpha}_1^2\right)^2 + \left(f_y\dot{\alpha}_1 + M\ddot{\alpha}_1\right)^2}, \\
a_2 &= \frac{mr\left[\left(k_y - M\dot{\alpha}_2^2\right)\dot{\alpha}_2^2 + \left(f_y\dot{\alpha}_2 + M\ddot{\alpha}_2\right)\ddot{\alpha}_2\right]}{\left(k_y - M\dot{\alpha}_2^2\right)^2 + \left(f_y\dot{\alpha}_2 + M\ddot{\alpha}_2\right)^2}, \\
a_3 &= \frac{mr\left[\left(k_y - M\dot{\alpha}_1^2\right)\dot{\alpha}_1^2 - \left(f_y\dot{\alpha}_1 + M\ddot{\alpha}_1\right)\ddot{\alpha}_1\right]}{\left(k_y - M\dot{\alpha}_1^2\right)^2 + \left(f_y\dot{\alpha}_1 + M\ddot{\alpha}_1\right)^2}, \\
a_4 &= \frac{mr\left[\left(k_y - M\dot{\alpha}_2^2\right)\dot{\alpha}_2^2 - \left(f_y\dot{\alpha}_2 + M\ddot{\alpha}_2\right)\ddot{\alpha}_2\right]}{\left(k_y - M\dot{\alpha}_2^2\right)^2 + \left(f_y\dot{\alpha}_2 + M\ddot{\alpha}_2\right)^2}.
\end{aligned} \tag{2}$$

The equations (1) and (2) has the coupling items: α_1, α_2, $\Delta\alpha_1$, and $\Delta\alpha_2$, which are symmetrically distributed in the dynamic formula, indicating that the minor variation of

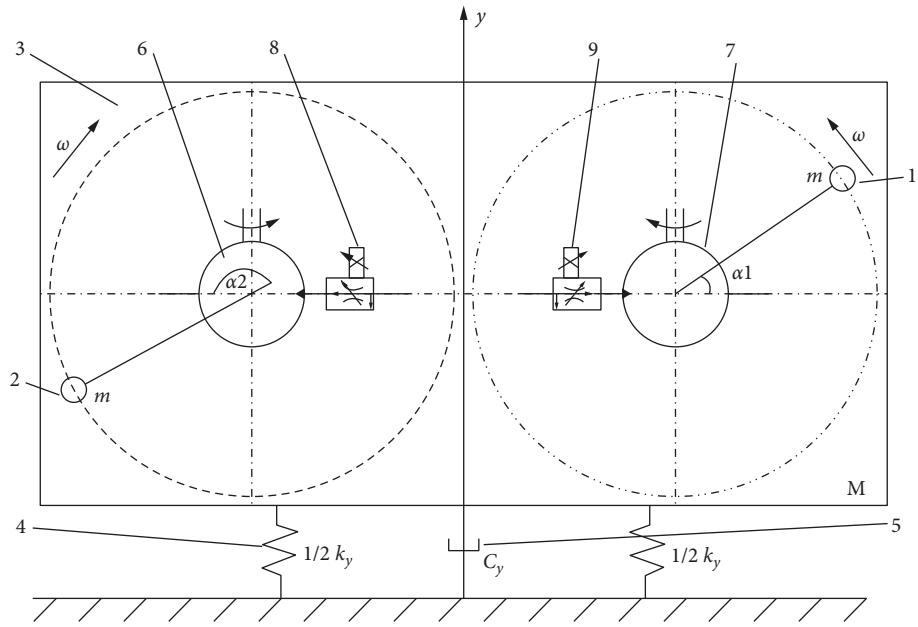

FIGURE 1: New vibration piling hammer-soil model. (1), (2) Eccentric blocks 1 and 2. (3) Pile hammer body. (4) Foundation soil's flexibility. (5) Foundation soil's damping. (6), (7) Hydraulic motors 6 and 7. (8), (9) Electrohydraulic proportional valves 8 and 9.

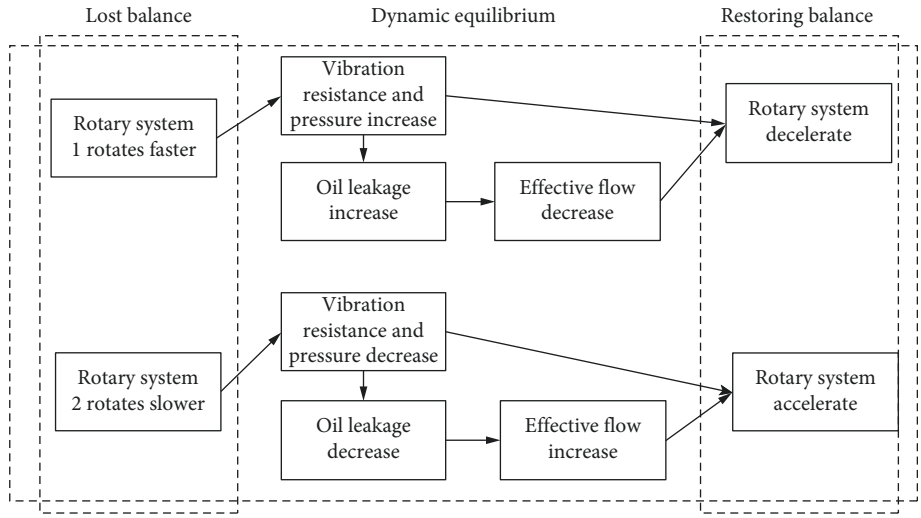

FIGURE 2: Dynamic balancing process of the two rotary systems in the hydraulic system.

rotational motion in the two rotating systems are mutually limited. The value of a_i ($i = 1$–4) is determined by the structure parameters of the vibration system and external conditions, such as M (mass of the whole vibration system), K_y (synthesis stiffness of foundation soil and isolation spring) [18], and so on, which indicate the influence of the oscillatory system on the strength of the vibration coupling between the exciters.

3.2. Mathematical Model of Leakage of Hydraulic Motor. As shown in Figure 3, the internal leakage of the motor is determined mainly by three factors in the working operation of the slanting axial piston motor, which are the plunger pair leakage, the slipper pair leakage, and the Port Plate leakage, respectively [19–21].

The piston pair has a matching gap and there is a high-pressure difference between the two ends of the piston ring. When the plunger moves to and from, the oil liquid in the column plug will leak from the piston pair clearance to the motor shell under the action of pressure difference. Figure 4 shows a schematic of the plunger pair.

The instantaneous leakage flow of a single piston pair is

$$Q_{l1i} = \frac{\pi d \delta_1^3}{12\eta l}\left(1 + \varepsilon^2\right)P_{Li} - \frac{\pi \mathrm{d}\delta_1}{2}v \quad i = 1, 2,$$
$$v = -\frac{D}{2}\sin\theta\,\dot{\psi}_i \sin\psi_i \quad i = 1, 2. \tag{3}$$

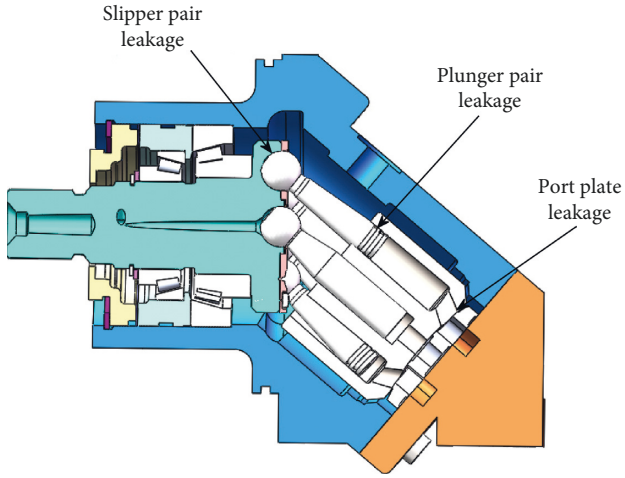

Figure 3: Internal leakage diagram of the axial piston motor.

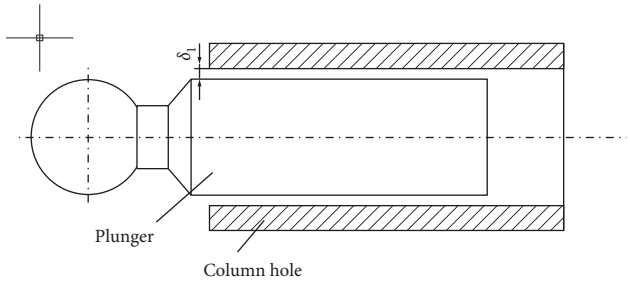

Figure 4: Plunger pair.

The leakage of the motor is mainly caused by the leakage of the piston pair, but the leakage of the Port Plate and the slipper should not be ignored either. The leakage flow of the slipper pair is as follows:

$$Q_{l2i} = \frac{\pi\delta_2^3}{6\eta In(R_2/R_1)} \cdot \lambda P_{Li} \quad i = 1, 2. \tag{4}$$

The leakage flow of the Port Plate as follows:

$$Q_{l3i} = \frac{\pi\delta_3^3}{6\eta}\left(\frac{1}{In(R_6/R_8)} + \frac{1}{In(R_7/R_5)}\right)(\varphi_2 - \varphi_1) \cdot \lambda P_{Li} \quad i = 1, 2. \tag{5}$$

The total leakage of oil in slanting axial piston motor is as follows:

$$Q_{Li} = Q_{l1i} + Q_{l2i} + Q_{l3i}. \tag{6}$$

3.3. The Derivation of Coupling Characteristic Solution. Hydraulic pressure energy drives eccentric block to rotate, and then convert into mechanical energy. The energy conversion relationship is as follows:

$$p_i Q_i = T_i \dot{\alpha}_i.$$
$$\dot{\alpha}_i = \omega_{0i} + \Delta\dot{\alpha}_i \quad i = 1, 2. \tag{7}$$

In the equation above, p_i stands for the oil pressure, Q_i for effective instantaneous flow, and $\dot{\alpha}_i$ for the instantaneous angular velocity.

$$T_i = \frac{p_i Q_i}{\dot{\alpha}_i}, \quad i = 1, 2. \tag{8}$$

Because the electrohydraulic proportional valve was directly fixed at the inlet of the hydraulic motor, under the control of the proportional valve, the working flow into the two motors is equal; so, high accuracy of angular velocity ω_{01}, ω_{02} can be achieved (the range of error can be controlled within 2%). Therefore, it can be assumed that

$$\omega_{01} = \omega_{02} = \omega_0. \tag{9}$$

Substituting equations (8) and (9) in equation (1) gives

$$\begin{aligned} E_{f_1} &= \frac{2f_1}{mr^2}, \\ E_{f_2} &= \frac{2f_2}{mr^2}, \\ E_{\mu_1} &= \frac{2\mu_1}{m\omega_0 r^2} \\ E_{\mu_2} &= \frac{2\mu_2}{m\omega_0 r^2}, \\ E_k &= \frac{2a_2\omega_0}{r}, \\ E_c &= \frac{2a_3\omega_0}{r}. \end{aligned} \tag{10}$$

Then, we can get

$$\begin{aligned} &\Delta\ddot{\alpha}_1 + \left(E_{f_1} - E_c + \frac{E_{\mu_1}}{\omega_0} Q_1 p_1\right)\Delta\dot{\alpha}_1 + (E_k \sin\gamma - E_c \cos\gamma)\Delta\dot{\alpha}_2 \\ &+ \frac{1}{2}E_k\omega_0 \sin\gamma + E_{f_1}\omega_0 - \frac{1}{2}E_c\omega_0 - \frac{1}{2}E_c\omega_0 \cos\gamma \\ &- E_{\mu_1} Q_1 p_1 = 0, \\ &\Delta\ddot{\alpha}_2 - (E_k \sin\gamma + E_c \cos\gamma)\Delta\dot{\alpha}_1 + \left(E_{f_2} - E_c + \frac{E_{\mu_2}}{\omega_0} Q_2 p_2\right)\Delta\dot{\alpha}_2 \\ &- \frac{1}{2}E_k\omega_0 \sin\gamma + E_{f_2}\omega_0 - \frac{1}{2}E_c\omega_0 - \frac{1}{2}E_c\omega_0 \cos\gamma \\ &- E_{\mu_2} Q_2 p_2 = 0. \end{aligned} \tag{11}$$

In equation (10), under the condition of certain structural parameters about vibration pile and certain angular frequency ω_0, E_{f1} and E_{f2} are only determined by mechanical transfer resistance coefficient of gyration systems 1 and 2; $E_{\mu 1}$ and $E_{\mu 2}$ are only determined by mechanical efficiency of the hydraulic motor; E_k is only related to stiffness of foundation soil; and E_c is only related to damping of foundation soil.

The equation (11) describes the changes about micro-angle $\Delta\alpha_1$, $\Delta\alpha_2$ within a cycle. Suppose the foundation soil

characteristic parameters are non-time-variable. Under the condition that gyration speed ω_0 is approximately constant, it is a second-order nonlinear equation with constant coefficients. Considering the periodic motion within one cycle, the singularity equation in the phase plane ($\Delta\alpha_1$, $\Delta\alpha_2$) consisted by equation disaggregation is

$$\begin{aligned}
&\Delta\ddot{\alpha}_1 + \left(E_{f_1} - E_c + \frac{E_{\mu_1}}{\omega_0} Q_1 p_1\right)\Delta\dot{\alpha}_1 + (E_k \sin\gamma - E_c \cos\gamma)\Delta\dot{\alpha}_2 \\
&\quad + \frac{1}{2}E_k\omega_0 \sin\gamma + E_{f_1}\omega_0 - \frac{1}{2}E_c\omega_0 - \frac{1}{2}E_c\omega_0 \cos\gamma \\
&\quad - E_{\mu_1} Q_1 p_1 = 0, \\
&\Delta\ddot{\alpha}_2 - (E_k \sin\gamma + E_c \cos\gamma)\Delta\dot{\alpha}_1 + \left(E_{f_2} - E_c + \frac{E_{\mu_2}}{\omega_0} Q_2 p_2\right)\Delta\dot{\alpha}_2 \\
&\quad - \frac{1}{2}E_k\omega_0 \sin\gamma + E_{f_2}\omega_0 - \frac{1}{2}E_c\omega_0 - \frac{1}{2}E_c\omega_0 \cos\gamma \\
&\quad - E_{\mu_2} Q_2 p_2 = 0.
\end{aligned} \tag{12}$$

Disappearing items of equations (12) and symmetrical reorganizing, we can get the solution to the equation as follows:

$$\begin{aligned}
\Delta\dot{\alpha}_1 &= \frac{\overline{\Delta\dot{\alpha}'}}{H} + \frac{\Delta\dot{\alpha}'}{H}, \\
\Delta\dot{\alpha}_2 &= \frac{\overline{\Delta\dot{\alpha}'}}{H} - \frac{\Delta\dot{\alpha}'}{H}.
\end{aligned} \tag{13}$$

In equation (13),

$$\begin{aligned}
H &= E_k^2 \sin^2\gamma - E_c^2 \cos^2\gamma + E_{f_1}E_{f_2} - 2E_c\overline{E_f} + {E_c}^2 \\
&\quad + \frac{1}{\omega_0}\left(2\overline{E_f}\,\overline{N} - \frac{\Delta E_f}{2}\Delta N - 2E_c\overline{N}\right) + \frac{N_1 N_2}{{\omega_0}^2}, \\
\overline{\Delta\dot{\alpha}'} &= -\frac{1}{2}E_k^2 \sin^2\gamma\omega_0 + \frac{1}{2}E_c^2\omega_0 \cos^2\gamma - \frac{1}{4}E_k\omega_0\Delta E_f \sin\gamma \\
&\quad - E_{f_1}E_{f_2}\omega_0 - \frac{1}{2}E_c^2\omega_0\frac{1}{2}E_c\omega_0 \cos\gamma\overline{E_f} + \frac{3}{2}E_c\omega_0\overline{E_f} \\
&\quad + \frac{3}{4}E_k \sin\gamma\Delta N + \frac{3}{2}E_c\overline{N}\cos\gamma - \frac{1}{2}E_c\overline{N} + \frac{N_1 N_2}{\omega_0}, \\
\Delta\dot{\alpha}' &= \frac{1}{2}E_k\omega_0\overline{E_f} \sin\gamma + \frac{1}{4}E_c\omega_0\Delta E_f \cos\gamma + \frac{1}{4}E_c\omega_0\Delta E_f \\
&\quad - \frac{3}{2}E_k\overline{N}\sin\gamma - \frac{3}{4}E_c\Delta N\cos\gamma - \Delta E_f\overline{N} + \overline{E_f}\Delta N \\
&\quad - \frac{3}{4}E_c\Delta N,
\end{aligned} \tag{14}$$

In equation (14),

$$\begin{aligned}
\Delta E_f &= E_{f_1} - E_{f_2}, \\
\overline{E_f} &= \frac{E_{f_1} + E_{f_2}}{2} \\
E_{f_1} &= \overline{E_f} + \frac{\Delta E_f}{2}, \\
E_{f_2} &= \overline{E_f} - \frac{\Delta E_f}{2},
\end{aligned} \tag{15}$$

$$\begin{aligned}
\overline{N} &= \frac{N_1 + N_2}{2}, \\
\Delta N &= N_1 - N_2,
\end{aligned} \tag{16}$$

and

$$\begin{aligned}
N_1 &= E_{\mu_1}Q_1 p_1 = \overline{N} + \frac{\Delta N}{2}, \\
N_2 &= E_{\mu_2}Q_2 p_2 = \overline{N} - \frac{\Delta N}{2}.
\end{aligned} \tag{17}$$

Equations (13) and (14) include not only the situation of the power consumed by the eccentric block at any position within one circle, but also the symmetry of the angular velocity of eccentric gyration between systems 1 and 2, and the mutual energy consumption characteristics.

In equation (17), Q_1, Q_2 are the effective instantaneous flow of the hydraulic motors 1 and 2, which constitute the total flow of the hydraulic motor with the leakage flow through the electromagnetic proportional valve to the hydraulic motor.

$$\begin{aligned}
Q_1 &= Q - Q_{L1}, \\
Q_2 &= Q - Q_{L2},
\end{aligned} \tag{18}$$

then,

$$\begin{aligned}
N_1 &= E_{\mu_1}P_1 Q - E_{\mu_1}P_1^2\left(w\delta_{11}^3 + u\delta_{12}^3 + v\delta_{13}^3\right), \\
N_2 &= E_{\mu_2}P_2 Q - E_{\mu_2}P_2^2\left(w\delta_{21}^3 + u\delta_{22}^3 + v\delta_{23}^3\right), \\
\Delta N &= \left(E_{\mu_1}P_1 - E_{\mu_2}P_2\right)Q - E_{\mu_1}P_1^2\left(w\delta_{11}^3 + u\delta_{12}^3 + v\delta_{13}^3\right) \\
&\quad + E_{\mu_2}P_2 2\left(w\delta_{21}^3 + u\delta_{22}^3 + v\delta_{23}^3\right), \\
\overline{N} &= \frac{1}{2}\left[\left(E_{\mu_1}P_1 + E_{\mu_2}P_2\right)Q - E_{\mu_1}P_1^2\left(w\delta_{11}^3 + u\delta_{12}^3 + v\delta_{13}^3\right)\right. \\
&\quad \left. - E_{\mu_2}P_2^2\left(w\delta_{21}^3 + u\delta_{22}^3 + v\delta_{23}^3\right)\right],
\end{aligned} \tag{19}$$

wherein

$$\begin{aligned}
w &= \frac{\pi d}{12\eta l}\left(1 + \varepsilon^2\right), \\
u &= \frac{\pi}{6\eta In\left(R_2/R_1\right)} \cdot \lambda, \\
v &= \frac{\pi}{6\eta}\left(\frac{1}{In\left(R_6/R_8\right)} + \frac{1}{In\left(R_7/R_5\right)}\right)(\varphi_2 - \varphi_1) \cdot \lambda.
\end{aligned} \tag{20}$$

4. Synchronous Criterion

The necessary criterion for synchronization is that there must exist a solution γ to equation (13), and it makes

$$\Delta\dot{\alpha}' = 0. \tag{21}$$

That is to say, the solution to equation (22) must exist [22].

$$\frac{1}{2}E_k\omega_0\overline{E_f}\sin\gamma + \frac{1}{4}E_c\omega_0\Delta E_f\cos\gamma + \frac{1}{4}E_c\omega_0\Delta E_f - \frac{3}{2}E_k\overline{N}\sin\gamma - \frac{3}{4}E_c\Delta N\cos\gamma - \Delta E_f\overline{N} + \overline{E_f}\Delta N - \frac{3}{4}E_c\Delta N = 0. \tag{22}$$

Equation (22) can be transformed into the following equation (23).

$$\left(\frac{1}{2}\omega_0\overline{E_f} - \frac{3}{2}\overline{N}\right)E_K\sin\gamma + \frac{1}{4}E_C\omega_0\Delta E_f(\cos\gamma + 1) - \frac{3}{4}E_C\Delta N(\cos\gamma + 1) - \Delta E_f\overline{N} + \overline{E_f}\Delta N = 0. \tag{23}$$

According to equations (15) and (16), the last two elements of equation (23) on the left side will be transformed into:

$$-\Delta E_f\overline{N} + \overline{E}_f\Delta N = -2E_{f_1}N_2 + 2E_{f_2}N_1. \tag{24}$$

In order to know the effect made by the gyration resistance coefficients f_1 and f_2 of rotating shafts 1 and 2 for synchronization, we can set the last two elements of equation (23) on the left side at 0. And, both sides of equation (24) will be 0.

$$-2E_{f_1}N_2 + 2E_{f_2}N_1 = 0. \tag{25}$$

According to the definition of equation (10), we can know that the sufficient condition for the establishment of equation (25) is that the discrepancy between the gyration resistance coefficients f_1 and f_2 is 0.

In this way, equation (23) is simplified into the following equation (26).

$$\left(\frac{1}{2}\omega_0\overline{E_f} - \frac{3}{2}\overline{N}\right)E_K\sin\gamma + \frac{1}{4}E_C\omega_0\Delta E_f(\cos\gamma + 1) - \frac{3}{4}E_C\Delta N(\cos\gamma + 1) = 0, \tag{26}$$

$$\text{Let } \begin{matrix} A = \left(\frac{1}{2}\omega_0\overline{E_f} - \frac{3}{2}\overline{N}\right)E_K \\ B = \left(\frac{1}{4}\omega_0 E_f - \frac{3}{4}N\right)E_C \end{matrix}. \tag{27}$$

Then, the trigonometric solution to equation (26) is

$$\cos\gamma = \frac{A^2 - B^2}{A^2 + B^2}. \tag{28}$$

So, the necessary criterion for the solution to synchronous equation (23) is

$$|\cos\gamma| \le 1. \tag{29}$$

Consequently, the solution γ exists.

That is to say, the synchronous criterion is

$$\left|\frac{A^2 - B^2}{A^2 + B^2}\right| = \left|1 - \frac{2B^2}{A^2 + B^2}\right| < 1. \tag{30}$$

Obviously, inequality (30) is always true. According to equation (25), we can know the meaning of equation (30) is that under the precondition that the gyration resistance coefficient, f_1 and f_2 are both 0, the gyration systems 1 and 2 will always be in sync regardless of structural parameters and gyration speed. So, reducing the gyration resistance coefficient of the gyration shaft is the most effective way to ensure the synchronous criterion. The conclusion is fully consistent with that of reference [3] obtained through electrohydraulic system-coupling modeling and simulation.

The discussion above is a special case for synchronous criterion where the gyration resistance coefficient is 0. Then, the case was considered that gyration resistance coefficient is not 0.

Equation (23) can be transformed into

$$A\sin\gamma + B(\cos\gamma + 1) + C = 0,$$

$$\text{Let } C = -\Delta E_f\overline{N} + \overline{E_f}\Delta N, \qquad \sin\beta = \frac{B}{\sqrt{A^2 + B^2}}. \tag{31}$$

Then, the trigonometric solution to equation (31) is

$$\sin(\gamma + \beta) = -\frac{B + C}{\sqrt{A^2 + B^2}}, \qquad \text{Set } D = -\frac{B + C}{\sqrt{A^2 + B^2}}. \tag{32}$$

The necessary condition for synchronous criterion is

$$\left|-\frac{B + C}{\sqrt{A^2 + B^2}}\right| \le 1. \tag{33}$$

If $C = 0$, the sufficient condition for equation (25) is true, equation (33) can be transformed into

$$\sin(\gamma + \beta) = \frac{-B}{\sqrt{A^2 + B^2}}. \tag{34}$$

Substitute equation (33) in equation (34), and then we get the solutions

$$\gamma = -2\beta \text{ or } \gamma = -180^\circ. \tag{35}$$

It shows that under the precondition that the gyration resistance coefficient is 0, the gyration systems 1 and 2 can keep constant sync with a phase difference near π or -2β, regardless of structural parameters, foundation soil stiffness, damping, and changes in the frequency. This conclusion is exactly the same as the one expressed by equation (30).

The algebraic expression D in equation (34) can be described as synchronous index. The absolute value of D can indicate the synchronous level for the strength of the vibration of the machine. The smaller $|D|$ is (that is, the smaller the synchronous phase difference γ is), the easier synchronization is, and the lighter the control system "burden" is.

5. Sensitivity Analysis on Factors Affecting System Synchronization

According to the derivation of the system-coupling synchronization criterion, there are several factors that affect the coupling synchronism of the system, including mainly the difference in the structural parameters between the two rotation systems, the internal leakage of two hydraulic motors, and the parameters of the foundation soil as the load. According to the criteria, the higher the system synchronization is, the smaller the phase difference value between the two eccentric blocks is.

According to the operation procedure of the orthogonal experiment design method [23], take the phase difference $\Delta\alpha$ between the two eccentric blocks of two rotation systems as an index, and take the difference between the rotary resistance coefficient of two motors Δf, the difference between the motor plunger value $\Delta\delta_1$, the synthetic stiffness of the foundation soil K_y, and the hydraulic system oil temperature T as factors affecting the index. The orthogonal experiment contains four factors, each containing five levels as follows (Table 1):

Table 1: Orthogonal factor levels.

Factor	$\Delta\delta_1$ (mm)	T(°C)	Δf (%)	K_y (N/m)
1	1.0×10^{-6}	45	2	1.4×10^{8}
2	1.5×10^{-6}	50	4	2.0×10^{8}
3	2.0×10^{-6}	55	6	2.6×10^{8}
4	2.5×10^{-6}	60	8	3.2×10^{8}
5	3.0×10^{-6}	65	10	3.8×10^{8}

Orthogonal table was selected as the orthogonal experimental design. The results are as follows (Table 2).

Table 2: Orthogonal results.

Program	$\Delta\delta_1$(mm)	T (°C)	Δf (%)	K_y (N/m)	$\Delta\alpha$ (rad)
1	1.0×10^{-6}	45	2	1.4×10^{8}	2.538
2	1.0×10^{-6}	50	4	2.0×10^{8}	2.057
3	1.0×10^{-6}	55	6	2.6×10^{8}	2.946
4	1.0×10^{-6}	60	8	3.2×10^{8}	3.340
5	1.0×10^{-6}	65	10	3.8×10^{8}	3.516
6	1.5×10^{-6}	45	4	2.6×10^{8}	3.083
7	1.5×10^{-6}	50	6	3.2×10^{8}	2.973
8	1.5×10^{-6}	55	8	3.8×10^{8}	4.418
9	1.5×10^{-6}	60	10	1.4×10^{8}	4.503
10	1.5×10^{-6}	65	2	2.0×10^{8}	3.112
11	2.0×10^{-6}	45	6	3.8×10^{8}	2.833
12	2.0×10^{-6}	50	8	1.4×10^{8}	2.059
13	2.0×10^{-6}	55	10	2.0×10^{8}	3.131
14	2.0×10^{-6}	60	2	2.6×10^{8}	3.109
15	2.0×10^{-6}	65	4	3.2×10^{8}	2.964
16	2.5×10^{-6}	45	8	2.0×10^{8}	2.905
17	2.5×10^{-6}	50	10	2.6×10^{8}	2.526
18	2.5×10^{-6}	55	2	3.2×10^{8}	2.829
19	2.5×10^{-6}	60	4	3.8×10^{8}	3.169
20	2.5×10^{-6}	65	6	1.4×10^{8}	3.154
21	3.0×10^{-6}	45	2	3.8×10^{8}	3.290
22	3.0×10^{-6}	50	4	2.0×10^{8}	3.077
23	3.0×10^{-6}	55	6	2.6×10^{8}	4.385
24	3.0×10^{-6}	60	8	3.2×10^{8}	3.017
25	3.0×10^{-6}	65	10	1.4×10^{8}	3.106

The range analysis of Table 2 was performed, and the average phase difference $\Delta\alpha$ between two eccentric blocks under the influence of various factors and the sensitivity arrangement order of each factor were obtained, as shown in Table 3.

Table 3: Range analysis results.

Factor	$\Delta\delta_1$	T	Δf	K_y
K_{1j}	1.150	1.121	1.390	0.854
K_{2j}	1.038	1.287	1.056	0.907
K_{3j}	1.064	1.106	1.148	0.615
K_{4j}	1.139	1.103	1.195	1.016
R_j	0.294	0.110	0.418	0.073
Sensitivity	2	3	1	4

From the mean average R_j value of the above table, the difference between the rotary resistance coefficient of two motors Δf had the greatest impact on the system synchronization, accounting for 46.7% of the four influencing factors, followed by the difference between the motor plunger value $\Delta\delta_1$ and the hydraulic system oil temperature T, which accounted for 32.8% and 12.3% of the four influencing factors, respectively. The synthetic stiffness K_y of foundation soil had the weakest influence on the synchronization of the system, accounting for 8.2%, and the sensitivity was the lowest.

Measures to improve synchronization are given as follows.

It can be seen from the above study what sensitivity factors affect system synchronization, and correspondingly the following measures can be taken to improve synchronization:

(1) The difference between the rotary resistance coefficient of two motors Δf had the greatest influence on synchronization, accounting for 46.7% of the impact percentage. Therefore, reducing the difference between the rotary resistance coefficient of two motors Δf or minimizing the rotary resistance coefficient of two motors is the most effective way to achieve system synchronization.

(2) Secondly, as the difference between the motor plunger value $\Delta\delta_1$ had a great influence on the synchronization, accounting for 32.8% of the impact percentage, improving the manufacturing and processing quality of the two eccentric rotor systems and reducing the structural difference, especially the difference between the motor plunger value, can significantly improve the synchronization.

(3) Temperature also affected system synchronization, accounting for 12.3% of the impact; consequently, reducing the temperature difference between the two systems is also very important.

(4) The stiffness of foundation soil had the weakest influence on system synchronization, accounting for 8.2% of the impact percentage, which indicates that the influence of different foundation soils on the system synchronization is relatively weak, and the coupling synchronization vibration hammer can adapt to different construction environments.

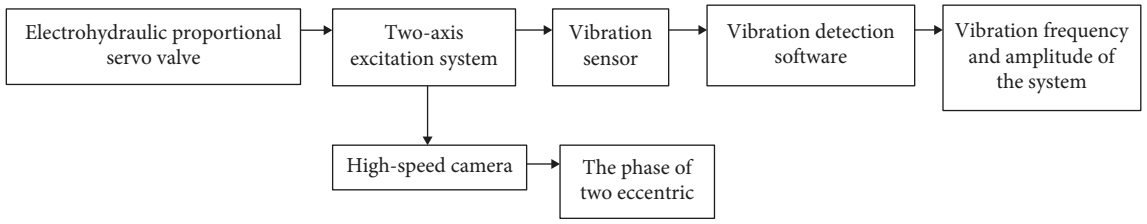

Figure 5: Test process.

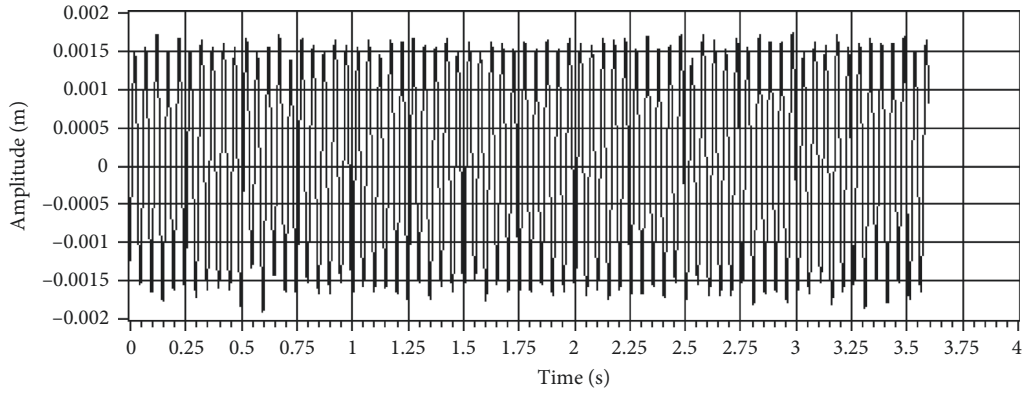

Figure 6: y-t curve, with $mr = 11$ kg·m.

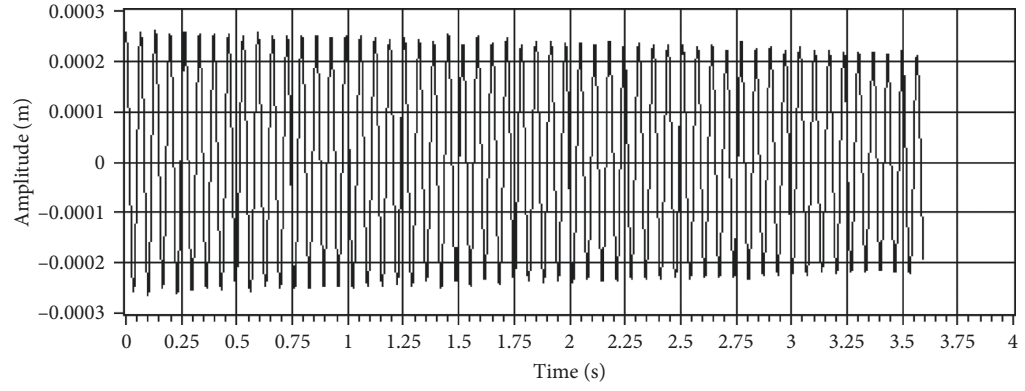

Figure 7: y-t curve, with $mr = 15$ kg·m.

6. Experiment

6.1. Change the Value of mr to Decrease B in the Synchronization Criterion. Test flowchart is shown in Figure 5.

The main testing devices include ZZYY40 experimental hydraulic vibrating pile hammer, 2 sets of steel plate to display the angle of the eccentric rotary shaft, 1 set of vibration detector and its software, 1 set of high-speed cameras, etc.

Figure 6 shows the amplitude detection results under the given vibration pile condition, wherein $mr = 11$ kg·m and $|D| = 0.65$ were obtained after calculation. According to the theoretical criterion, the synchronization evaluation index is less than what satisfies the synchronization criterion. Figure 6 shows the experimental result that the amplitude was stable near 0.0015 m, so the synchronization was realized. The experiment results correspond to the theoretical analysis.

Figure 7 shows the amplitude detection results under the given vibration pile condition, wherein $mr = 15$ kg·m, the other conditions are the same as the test conditions in Figure 6, and $|D| = 1.28$ was obtained after calculation. According to the theoretical criterion, the synchronization evaluation index is more than 1, which fails to satisfy the synchronization criterion. Figure 7 shows the experimental result that the amplitude gradually decreased from the initial value of 0.00025 m. High-speed camera was used to shoot steel plate for displaying the angle of eccentric rotating axis, 10 shooting photos in 1 second. The results showed that the phase difference between two eccentric blocks changed without following the same pattern. The experiment results corresponded to the theoretical analysis.

We also verified the synchronization criterion by adjusting the vibration frequency and the friction coefficient of the rotating system. All the experiments show that the synchronous evaluation model of the hydraulic-driven

Table 4: The first group of dimensional tolerance table of the testing motor plunger pair.

First group		Motor A tolerance (mm)	Motor B tolerance (mm)
Plunger pair 1	Plunger	−0.011	−0.013
	Hole	+0.010	+0.009
Plunger pair 2	Plunger	−0.015	−0.010
	Hole	+0.006	+0.012
Plunger pair 3	Plunger	−0.011	−0.010
	Hole	+0.012	+0.011
Plunger pair 4	Plunger	−0.012	−0.014
	Hole	+0.013	+0.008
Plunger pair 5	Plunger	−0.013	−0.015
	Hole	+0.009	+0.008
Plunger pair 6	Plunger	−0.014	−0.012
	Hole	+0.007	+0.010
Plunger pair 7	Plunger	−0.010	−0.011
	Hole	+0.015	+0.012

Table 5: The second group of dimensional tolerance table of the testing motor plunger pair.

Second group		Motor A tolerance (mm)	Motor B tolerance (mm)
Plunger pair 1	Plunger	−0.015	−0.012
	Hole	+0.005	+0.015
Plunger pair 2	Plunger	−0.010	−0.015
	Hole	+0.010	+0.012
Plunger pair 3	Plunger	−0.011	−0.013
	Hole	+0.010	+0.014
Plunger pair 4	Plunger	−0.013	−0.011
	Hole	+0.015	+0.015
Plunger pair 5	Plunger	−0.010	−0.015
	Hole	+0.010	+0.013
Plunger pair 6	Plunger	−0.013	−0.015
	Hole	+0.007	+0.012
Plunger pair 7	Plunger	−0.014	−0.014
	Hole	+0.006	+0.014

Figure 8: The plunger pair of Huade A2F80W2A2.

control system is correct, and the measures to improve the synchronization of the system are reasonable.

6.2. The Influence of the Difference between the Motor Plunger Value $\Delta\delta_1$ on System Synchronization. In this experiment, an optional matching method was used to match the Huade A2F80W2A2 slanting shaft plunger motor. The basic dimensions of the plunger and plunger holes are 18.9 mm. The dimensional tolerances of the plunger pairs selected from the two groups of motors are shown in Tables 4 and 5, and the physical picture is shown in Figure 8.

This experiment was based on the idea of single variable method, and only the difference in plunger pair clearance was changed. To make the other parameters as consistent as possible, the two groups of experiments were performed on the same test bench, and the system was cooled before starting the second group of experiments.

Experimental results: when the gap difference of plunger pair of double hydraulic motors was relatively smaller (group 1), although the phase difference value fluctuated greatly, its peak value stayed within a certain range and did not diverge. However, when the gap difference between the plunger pair of two hydraulic motors was larger (group 2), the phase difference was rapidly divergent, and its value increased constantly. The validity of the synchronization criterion and the sensitive factors affecting synchronization were verified.

7. Conclusions

The coupling items (α_1, α_2, $\Delta\alpha_1$, and $\Delta\alpha_2$) in equations (1) and (2) are symmetrically distributed in the dynamic formula, and according to the equations (13) and (14), the microangular velocity solution indicate that the minor variation of rotational motion in the two rotating systems is mutually limited.

The absolute value of synchronous index D, which is smaller than 1, can indicate the synchronous level for the strength of the vibration of machine. By analyzing the synchronous index D, it was found that the resistance coefficient difference and the difference in motor piston clearance have the greatest influence on the synchronous motion between the two motors. Of all the factors discussed in this paper, the influence of the resistance coefficient difference on system motion stability is the greatest, accounting for 46.7%, and the influence of the difference in motion pair structure (e.g. motor piston clearance) is the second, accounting for 32.8%.

For motors with a displacement of 80 ml/r, the condition of self-synchronization is that the difference in piston clearance between the two motors is equal to or smaller than 6 μm.

Symbols

K_y: synthesis stiffness of foundation soil and isolation spring
M: mass of the whole vibration system
f_y: foundation soil damping coefficient
m, r: mass and radius of the eccentric block
α_i: phase angle of each gyration eccentric block
f_i: gyration resistance coefficient
T_{Mi}: effective torque
μ_i: mechanical efficiency
p_i: working pressure
q_i: the effective displacement
ω_{0i}: steady-state gyration frequency
α_{0i}: steady-state gyration angle displacement
K_{Ci}: leakage coefficient
T_{Li}: the load torque
P_{Oi}: the load torque and pipeline back pressure of each hydraulic motor
$\Delta\alpha_i$: transient microangular displacement
$\Delta\dot{\alpha}_i$: instantaneous change of angular displacement
d: the diameter of the plunger
δ_1: clearance value of the plunger pair
η: dynamic viscosity of hydraulic oil
ε: plunger eccentricity
P_{Li}: motor load pressure
ψ_i: the angle of the plunger which rotates the motor
ι: engagement length of the plunger and the plunger pair
D: plunger distribution circle diameter
ν: the velocity of the plunger relative to the plunger hole
θ: motor swash plate inclination
δ_2: oil-film thickness of the slipper pair
R_1, R_2: radius value of slipper, radius value of the oil hole
λ: supply ratio, here set to 1
δ_3: oil film thickness of the Port Plate
$\delta_{ij(i=1,2;\ j=1,2,3)}$: the $\delta_{j(j=1,2,3)}$ of the hydraulic motor $i(i=1,2)$
R_5, R_6: inner seal ring radius of the Port Plate
R_7, R_8: outer seal ring radius of the Port Plate
Φ_1, Φ_2: hydrostatic bearing angle of the Port Plate.

Data Availability

The data used to support the findings of this study are included within the article.

Conflicts of Interest

All the authors declare that there are no conflicts of interest regarding the publication of this paper.

Acknowledgments

The authors thank the College of Mechanical and Electrical Engineering of CSU for supporting our research and all those who helped them with this article. The authors also thank the State Key Laboratory Independent Research Project (zzyjkt2014-08) and National High-tech R&D Program (863 Program 2013AA040203).

References

[1] I. I. Blekhman, *Synchronization in Science and Technology*, ASME PRESS, New York, NY, USA, 1988.

[2] B.-c. Wen, *Vibration Synchronization and Control Synchronization of Mechanical Systems*, Beijing Science Press, Beijing, China, 2003.

[3] C.-l. Luo, "Hydraulic vibratory pile hammer's pile driving dynamics and adjustment frequency and adjustment force moment control research," Doctoral Thesis, Central South University, Changsha, China, 2005.

[4] C. Luo, "Synchronization characteristics research of eccentric gyration system controlled by hydraulic driving," *Journal of Mechanical Engineering*, vol. 46, no. 6, pp. 176–181, 2010.

[5] I. I. Blekhman, A. L. Fradkov, O. P. Tomchina, and D. E. Bogdanov, "Self-synchronization and controlled synchronization: general definition and example design," *Mathematics and Computers in Simulation*, vol. 58, no. 4, pp. 367–384, 2002.

[6] Q.-k. Han, Z.-y. Qing, and B.-c. Wen, "Self-synchronization vibration system's stability and bifurcation," *Vibration and Shock*, vol. 26, no. 1, pp. 31–34, 2007.

[7] T. Zhang, B. Wen, and J. Fan, "Study on synchronization of two eccentric rotors driven by hydraulic motors in one vibrating system," *Shock and Vibration*, vol. 4, no. 5-6, pp. 305–310, 1997.

[8] C.-l. Luo, Z.-q. Tang, X. Mo, and Z.-y. Chen, "Leakage characteristics and coupling synchronization criterion of motor in hydraulic vibration hammer system without synchronous gear," *Journal of Central South University (Science and Technology)*, 2019, In press.

[9] D Wong, M.W. O'Neill, and C. Vipulanandan, "Modelling of vibratory pile driving in sand," *International journal for numerical and analytical methods in geomechanics*, vol. 16, no. 3, pp. 189–210, 2010.

[10] F. Rausche, "Modeling of vibratory pile driving," *Journal of Geotechnical Engineering*, vol. 3, no. 3, pp. 367–383, 2002.

[11] X. Lai and W. Xie, "Theoretical and experimental study on electromechanical coupling properties of multihammer synchronous vibration system," *Shock and Vibration*, vol. 3, pp. 1–11, 2016.

[12] He Li, Dan Liu, Ye Li, and Bang-chun Wen, "Self-Synchronous Theory of Novel No Swing Vibrating Mechanism Driven by Two Motors," *Journal of Northeastern University*, vol. 34, no. 10, pp. 1446–1450, 2013.

[13] H. Li, D. Liu, L. Jiang, C. Zhao, and B. Wen, "Self-synchronization theory of dual motor driven vibration system with two-stage vibration isolation frame," *Applied Mathematics and Mechanics*, vol. 36, no. 2, pp. 265–278, 2015.

[14] C.-l Luo, "Hydraulic vibratory pile hammer' adjustment force moment's new structure scheme and its characteristic analysis," *Rock Drilling Machinery Pneumatic Tool*, vol. 4, pp. 31–340, 2004.

[15] X. Chen, X. Kong, J. Dou et al., "Numerical and experimental investigation on self-synchronization of two eccentric rotors in the vibration system," *Biological Cybernetics*, vol. 101, no. 3, pp. 215–226, 2016.

[16] S. Li, S. Yang, and W. Guo, "Investigation on chaotic motion in hysteretic non-linear suspension system with multi-frequency excitations," *Mechanics Research Communications*, vol. 31, no. 2, pp. 229–236, 2004.

[17] M. Borowiec, G. Litak, and A. Syta, "Vibration of the Duffing oscillator: Effect of Fractional Damping," *Shock and Vibration*, vol. 14, pp. 29–36, 2007.

[18] Xue-liang Zhang, Bang-chun Wen, and Chun-yu Zhao, "Vibratory synchronization and coupling dynamic characteristics of multiple unbalanced rotors on a mass-spring rigid base," *International Journal of Non-Linear Mechanics*, vol. 28, no. 6, pp. 2049–2058, 2014.

[19] J. M. Bergada, D. L. Davies, S. Kumar, and J. Watton, "The effect of oil pressure and temperature on barrel film thickness and barrel dynamics of an axial piston pump," *Meccanica*, vol. 47, no. 3, pp. 639–654, 2011.

[20] J. M. Bergada, S. Kumar, D. L. Davies, and J. Watton, "A complete analysis of axial piston pump leakage and output flow ripples," *Applied Mathematical Modelling*, vol. 36, no. 4, pp. 1731–1751, 2012.

[21] B. Zhang, *Study on virtual prototype and pressure characterstics of oil film for axial piston pump*, Ph.D. thesis, Zhejiang University, Hangzhou, China, 2009.

[22] X.-L. Zhang, C.-Y. Zhao, and B.-C. Bang, "Theoretical and experimental study on synchronization of the two homodromy exciters in a non-resonant vibrating system," *Shock and Vibration*, vol. 20, no. 2, pp. 327–340, 2013.

[23] R.-j. Liu, Y.-w. Zhang, and C.-w. Wen, "Study on orthogonal test design and analysis method," *Experimental Technology and Management*, vol. 27, no. 9, pp. 52–55, 2010.